Investigating Ohmic Heating as a Solar Active Region Atmosphere Heating Mechanism

THE UNIVERSITY OF ALABAMA IN HUNTSVILLE
CENTER FOR SPACE PLASMA & AERONOMIC RESEARCH

Makayla Frisse[1], Mehmet Sarp Yalim[2]

[1]The University of Alabama in Huntsville, Department of Physics, Huntsville, AL, USA ; [2]The University of Alabama in Huntsville, Center for Space Plasma and Aeronomic Research, Huntsville, AL, USA

Introduction

One of the most compelling questions in modern solar physics is the cause of the extreme heating of the solar atmosphere, which causes a temperature increase from about 5,000 K in the photosphere to nearly 1 million K in the corona in just about 10,000 km. There are various mechanisms proposed to contribute to this heating. In this work, we investigate Ohmic heating due to the dissipation of electric currents by magnetic resistivity, namely Cowling resistivity, as a heating mechanism of the lower solar atmosphere, namely the chromosphere. The plasma in the chromosphere is not fully ionized and ions and neutrals exist simultaneously. Cowling resistivity follows the interactions between ions and neutrals, it is a function of the plasma bulk density ρ, temperature *T*, the magnetic field ***B***, as well as the ion and electron number densities, n_i and n_e. We perform a data-constrained analysis to calculate the Ohmic heating rate in a solar active region atmosphere based on tabulated data of stratified density and temperature profiles from five different semi-empirical solar atmosphere models in combination with observational magnetic field data.

Data

Observational data is from:

- Solar Dynamics Observatory (SDO) /Helioseismic and Magnetic Imager(HMI)
  - SHARP vector magnetogram data
- Dunn Solar Telescope (DST)/ Interferometric BI-dimensional Spectrometer (IBIS)
  - high-resolution spectroscopic Ca II data

Solar Atmosphere Models:

- Maltby M (Maltby et al., 1986)
  - models sunspot umbrae
- VAL C (Vernazza et al., 1981)
  - models the quiet sun
- VAL F (Vernazza et al., 1981)
  - models bright filament networks
- HSRA (Gingerich et al., 1971)
  - models the quiet sun
- Ding & Fang (Ding & Fang, 1989)
  - models sunspot penumbrae

We observe:

- National Oceanic and Atmospheric Administration (NOAA) active region (AR) 11166 on 2011-03-07 at 06:00:29 UT
  - HMI
- NOAA AR 12002 on 2014-03-13 at 20:48 UT and 21:00 UT
  - HMI & IBIS

Methods

Our method (Yalim et al., 2020) is based on the generalized Ohm's law relation given as follows:

$$Q = (\boldsymbol{E} + (\boldsymbol{v} \times \boldsymbol{B})) \cdot \boldsymbol{j} = \eta J_{\parallel}^2 + \boxed{\eta_C J_{\perp}^2}$$

where Q is frictional Joule (Ohmic) heating, **E** is the electric field, **v** is velocity, **B** is the magnetic field, **j** is the current density, η is the Coulomb resistivity, η_C is the Cowling resistivity, and $J_{//}$ and $J_{\perp}$ are the components of current density parallel and perpendicular to the magnetic field, respectively. We calculate the Cowling resistivity from

$$\frac{\xi_n^2 B_0^2}{\alpha_n} = \eta_C - \eta,$$

where $\xi_n = \frac{\rho_n}{\rho} = \frac{r}{1+r}$ is the neutral fraction for a hydrogen plasma, B_0 is the magnetic field strength, r is the ratio of the number density of neutrals to ions, and α_n is a factor expressed in terms of the effective collisional frequency (Braginskii 1965).

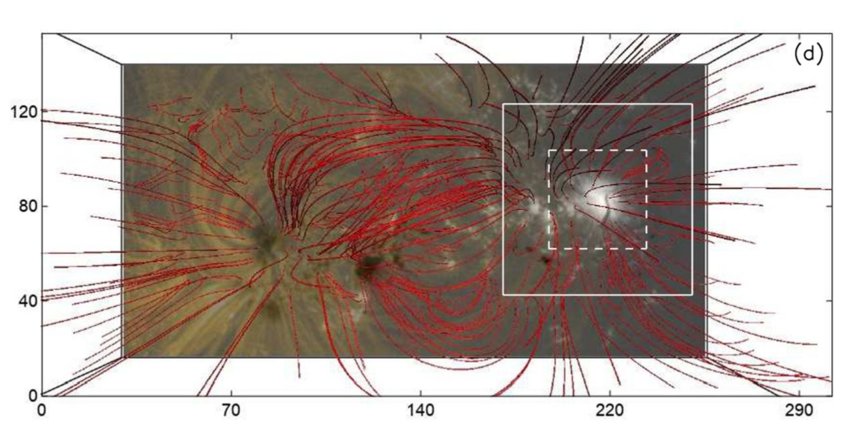

Figure 1. Field lines derived from the non-force-free field (NFFF) extrapolation overlaid on a composite image of the vertical component of the magnetic field and the AIA 171 Å image for the SHARP field of view(FOV) of AR 12002. The solid and dashed white squares correspond to the IBIS FOV and the smaller FOV shown in Fig. 9, respectively (Louis et al., 2021).

- To calculate the Cowling resistivity, we obtain T, ρ, n_i, and n_e from tabulated solar atmosphere data, and **B** field from non-force-free field (NFFF) extrapolation (Hu & Dasgupta 2008) applied to HMI SHARP magnetograms
- Calculate the Cowling resistivity from that result
- Calculate the electric currents from the magnetic field data
- Calculate the Ohmic heating rate based on η_C and currents
- Determine the average local & non local thermodynamic equilibrium temperatures (LTE & NLTE) from inverted IBIS data, across the light bridge in AR 12002

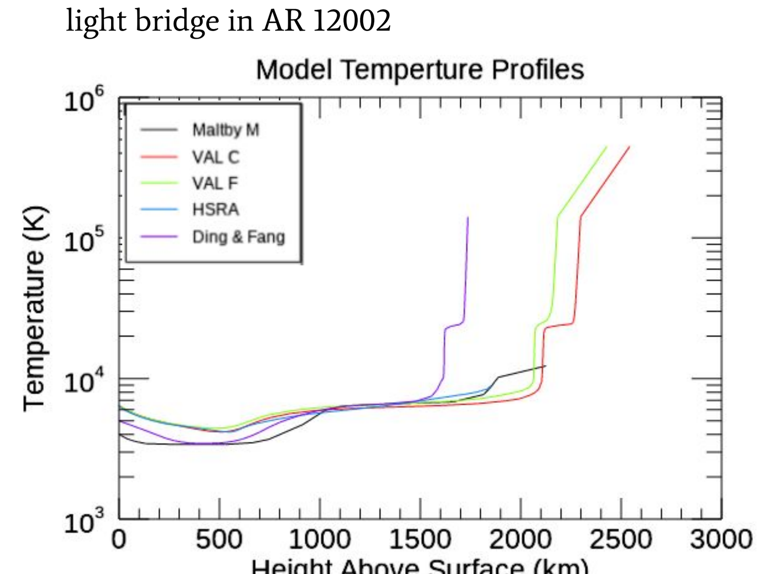

Figure 2. T profiles in the chromosphere obtained from all models.

Results

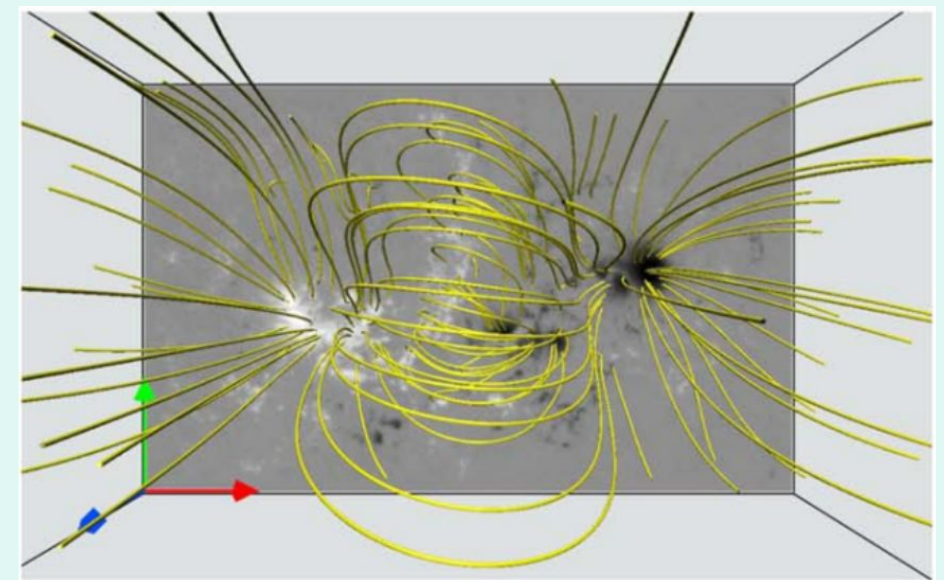

Figure 3. NFFF magnetic fieldlines showing AR 11166 (Yalim et al., 2020).

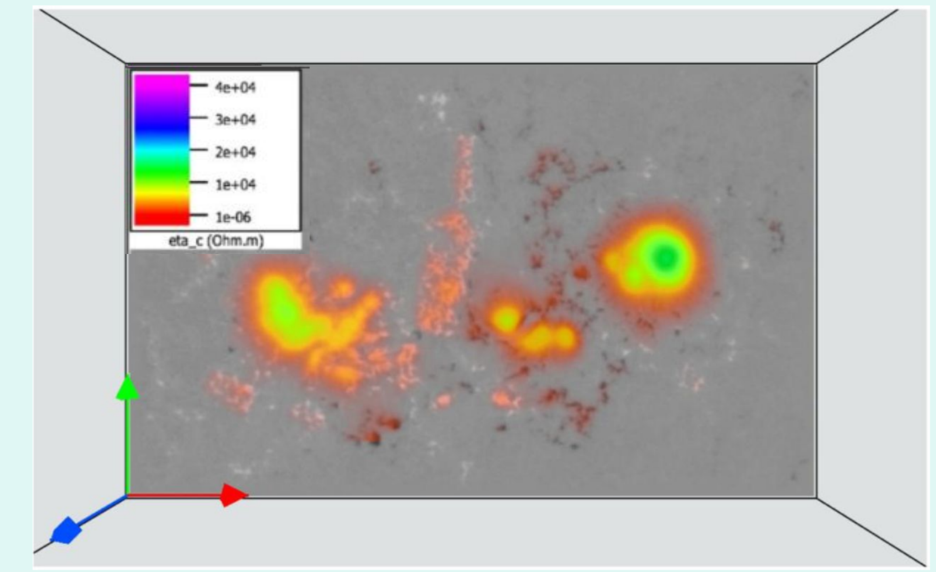

Figure 4. Direct volume rendering of η_C between 1 and 2 Mm height showing AR 11166 (Yalim et al., 2020).

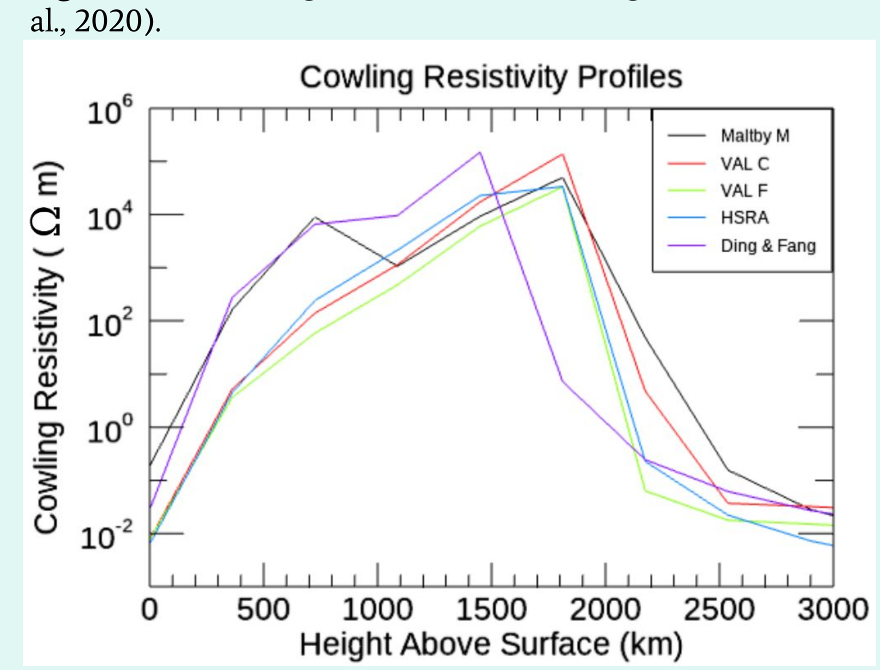

Figure 6. Variations of the maximum values of η_C profiles with height, from each of the five models, with HMI data from AR 11166.

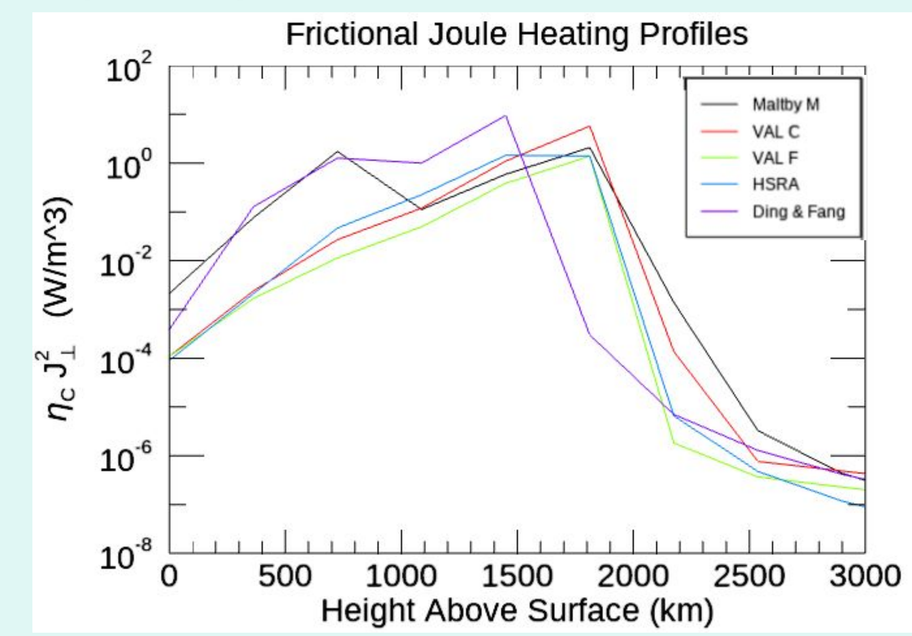

Figure 7. Variations of the maximum values of Joule heating profiles with height, from each of the five models, with HMI data from AR 11166.

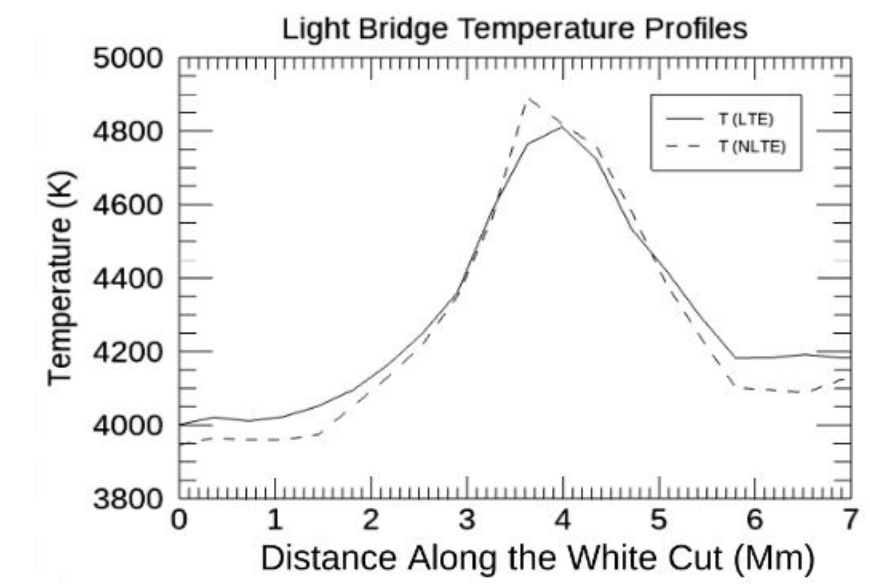

Figure 5. Horizontal variation in temperature, averaged in height, across the center of the LB at the white horizontal cut shown in Fig 9.

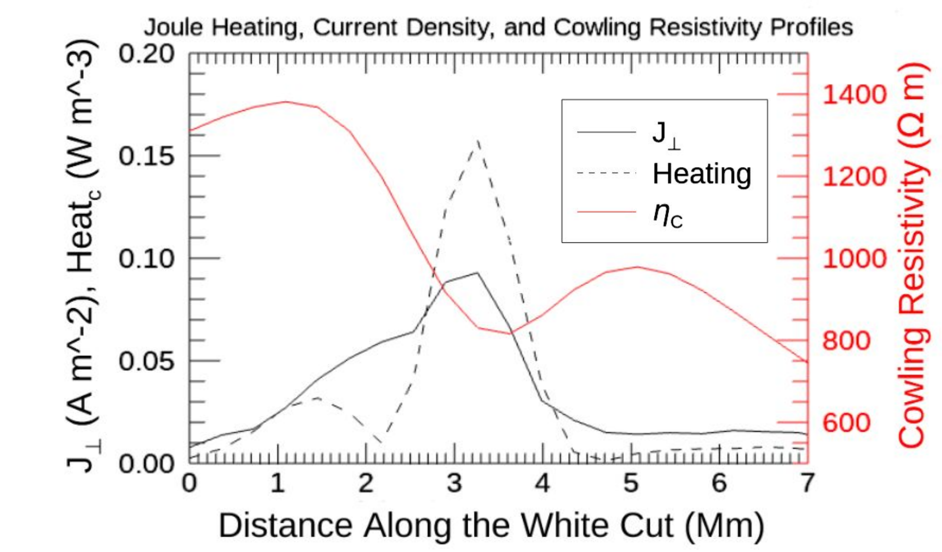

Figure 8. Horizontal variation of $J_\perp$, η_C, and the Joule heating along the white cut as in Fig. 9. $J_\perp$, η_C, and the Joule heating are averaged in height. η_C is calculated based on the Maltby M model. $J_\perp$ has been scaled up by a factor of three and the heating term has been reduced by a factor of two.

Total Joule Heating Rate Values between 0-2,500 km Height at the Maximum Height Averaged Heating Location on the Light Bridge across the White Cut in Figure 9 (W/m^3)

Model	Time (20:48 UT)	Time (21:00 UT)
Maltby M	1.2894	1.6812
VAL C	1.3542	1.8088
VAL F	0.3635	0.4848
HSRA	0.6846	0.9073
Ding & Fang	3.1060	4.0749

Table 1. The total Joule heating rate values between 0-2,500 km height at the maximum height averaged Joule heating location on the light bridge across the white cut in Figure 9 for each model at 20:48 and 21:00 UT for AR 12002.

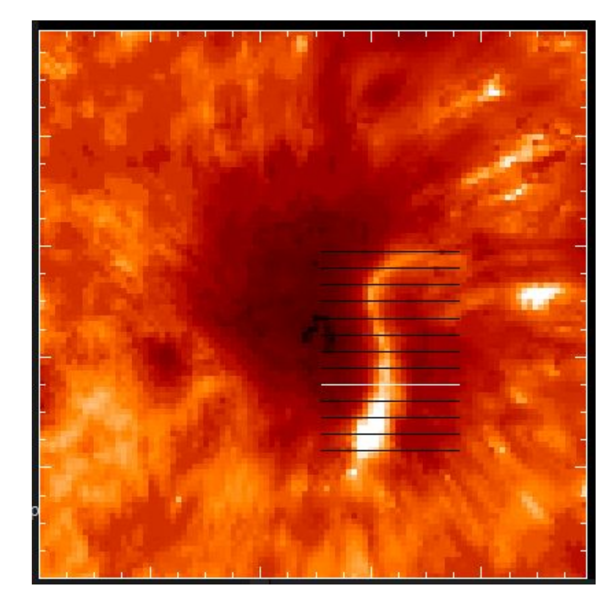

Figure 9. Sunspot light bridge in AR 12002 (Louis et al, 2021). The white horizontal line marks cut No. 5 used in Figs. 5, 8, and 10.

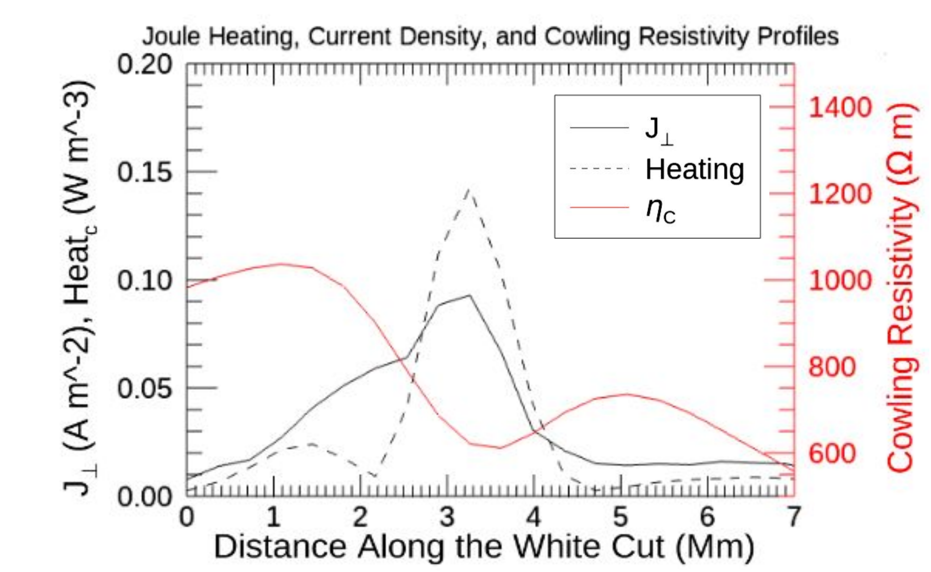

Figure 10. The same distribution as in Fig. 8 for the Ding & Fang model.

Discussion and Conclusions

- We consider two different sets of solar atmospheric models: Maltby M and Ding & Fang are sunspot atmosphere models and VAL C, VAL F, and HSRA are quiet Sun and plage models. The sunspot atmosphere being relatively cooler than the quiet Sun atmosphere can be observed from the T stratifications in Fig. 2.
- The strong quadratic dependence of Cowling resistivity to the magnetic field strength can be seen from the coinciding maximum η_C values with the sunspot locations in Fig. 4.
- In Figs. 6 & 7, we observe that both Ding & Fang and Maltby M models have an earlier peak for both η_C and Joule heating. This can be attributed to these models being of the penumbra and umbra, which are relatively cooler than the quiet Sun. As such, there are more neutrals present at lower heights in the former models. Cowling resistivity has a quadratic dependence on the neutral fraction, which is responsible for the higher values of η_C and the Joule heating.
- From Figs 5, 8, & 10, we observe an alignment of the LTE T, NLTE T, $J_\perp$, and heating peaks across the light bridge. This demonstrates a strong dependence of heating on current, because the heating makes a peak despite η_C has a local minimum at that location.
- From Table 1, we see that the total Joule heating at 21:00 UT is consistently greater than at 20:48 UT, and thus we may conclude that the light bridge experiences an ongoing heating event due to this mechanism.
- Also from Table 1, we see that VAL C and Ding & Fang lead to a greater total heating than Maltby M, and thus may be better for modeling the heating of ARs, in particular light bridges, despite Maltby M being the only umbral model. We need further quantitative validation for this conclusion.
- In future studies, we plan to calculate temperature and internal energy enhancements within the light bridge with respect to umbral surroundings for quantitative validation, and to repeat our entire analysis using observational temperature data from IBIS instead of the tabulated T data.

References

[1]Maltby, P., et al. 1986, ApJ, 306, 284
[2]Vernazza, J. E., etal. 1981, ApJS, 45, 635
[3]Gingerich, O., et al. 1971, Sol. Phys., 18, 347
[4]Ding, M. D. & Fang, C., 1989, A&A, 225, 204
[5]Yalim, M. S., at al. 2020, ApJ, 899, L4
[6]Braginskii, S. I. 1965, Transport processes in a Plasma, in Reviews of Plasma Physics, Vol. 1 (New York: Consultants Bureau)
[7]Louis, R. E., et al., 2021, A&A, 652, L4
[8]Hu, Q., & Dasgupta, B., 2008 Sol. Phys., 247, 87

Acknowledgments

I would like to thank Dr. M. Sarp Yalim for his support and guidance throughout the summer. The authors thank Dr. Christian Beck from National Solar Observatory, Dr. Avijeet Prasad from University of Oslo, Dr. Debi Prasad Choudhary from California State University Northridge, and Dr. Rohan E. Louis from Udaipur Solar Observatory for discussions and providing input files for the analysis. This work is supported by the NSF grant AGS-1950831 for the UAH/CSPAR and NASA/MSFC Heliophysics REU program. MSY acknowledges partial support from NSF award AGS-2020703. Any opinions, findings, and conclusions or recommendations expressed in this material are those of the author(s) and do not necessarily reflect the views of the National Science Foundation.